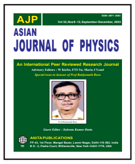

Asian Journal of Physics
Vol. 32, Nos 9-12 (2023) 559-571
Available on: www.asianjournalofphysics.com

ap

Sensitivity analysis of a double corrugated waveguide slow wave structure for a 151 - 161.5 GHz TWT*

Jeevan M Rao, Rupa Basu, Rosa Letizia, and Claudio Paoloni
School of Engineering, Lancaster University, Lancaster, LA1 4YW, United Kingdom

Dedicated to Prof B N Basu

TWTs at D-band (141 – 174.5 GHz) are the most promising solution to provide high transmission power for enabling long range wireless links with high capacity at sub-THz frequency. A D-band TWT was designed in the 151-161.5 GHz frequency band with about 10 W output power. The double corrugated waveguide is adopted as slow wave structure (SWS) for the relatively easy fabrication and alignment in comparison to other SWSs typically used at sub-THz frequency. Due to the short wavelength at D-band, the fabrication requires high precision computerised numerically controlled (CNC) milling machining and tight tolerance control. The sensitivity analysis of performance as a function of the dimensions of a device is an important method to predict in advance how the performance of the device is affected by geometry variations, and also to ascertain the required level of fabrication accuracy to meet the specifications. The sensitivity analysis is also useful to define the best initial dimensions for further optimization. This paper discusses the sensitivity analysis applied to the double corrugated waveguide (DCW) to be used in a 151-161.5 GHz TWT. A broad range of parameters are considered demonstrating the importance of fabrication accuracy and the eventual correction options for a correct functioning. The impact of fillets in the DCW pillars is also evaluated to eventually ease the fabrication requirement.

Keywords: Sub-THz, D-band, Traveling wave tube, Double corrugated waveguide, Sensitivity analysis.

DOI: 10.54955/AJP.32.9-12.2023.559-571

1 Introduction

The D-band with 27.5 GHz of allowed bandwidth for wireless links allocated in three different frequency bands in the range 141–174.5 GHz is potentially able to support links with tens of Gigabits per second (Gb/s) [1-3]. Numerous D-band front ends based on solid state power amplifiers (SSPAs) were reported in literature with high data rate but short transmission distance due to low transmission power [3]. The high free-space path-loss and attenuation, especially in rainy environment, requires transmission power of the order of a few Watts. This order of output power is not available from SSPAs.

Traveling wave tubes (TWTs) are the only amplifiers which are able to provide output power in the range of 10's of Watts at D-band [4-11]. TWTs at D-band are still State of the Art devices. The only working TWTs presented in literature are based on the folded waveguide [8,9]. The fabrication of the folded waveguide requires tight mechanical tolerances due to the high accuracy required to align the parts and their small dimensions.

* This paper contains some unpublished work of Jeevan M Rao, research associate at Lancaster University, who sadly passed away on 25th December 2020.

Corresponding author
e mail: c.paoloni@lancaster.ac.uk (Claudio Paoloni)

A different approach is the use of the double corrugated waveguide (DCW) as slow wave structure at D-band [6,12]. The DCW consists of two identical parallel rows of pillars to form a channel where the electron beam flows. When the two rows of pillars are sufficiently close together, they enhance the axial electric field in a quasi-circular shape to suitably interact with a circular electron beam. The DCW structure comprises of two blocks. The waveguide with the pillars is accommodated in one block. A second block is a flat surface closing the waveguide. This makes the alignment of the two blocks simple. The assembly is completed by the diffusion bonding of the two blocks together to form a robust structure from manufacturing point of view [6].

This paper presents a sensitivity analysis of the variation of different dimensions of the DCW such as width, pillar height, period and the electron beam position, that are important to assess the impact of the fabrication tolerances on the electrical performance of the structure.

2 D-band double corrugated waveguide design

A double corrugated waveguide has been designed in the band 151-161.5 GHz [11]. The single cell of the DCW is shown in Fig 1. Figure 2 shows the cross section and the top view. The nominal dimensions are listed in Table 1. The DCW is assumed to be used with 13.9 kV beam voltage. It may be noted that the cross-section of each pillar remains as small as 90 µm×90 µm (due to the short wavelength at the operation frequency). This tiny dimensions makes the fabrication process challenging requiring strict tolerances.

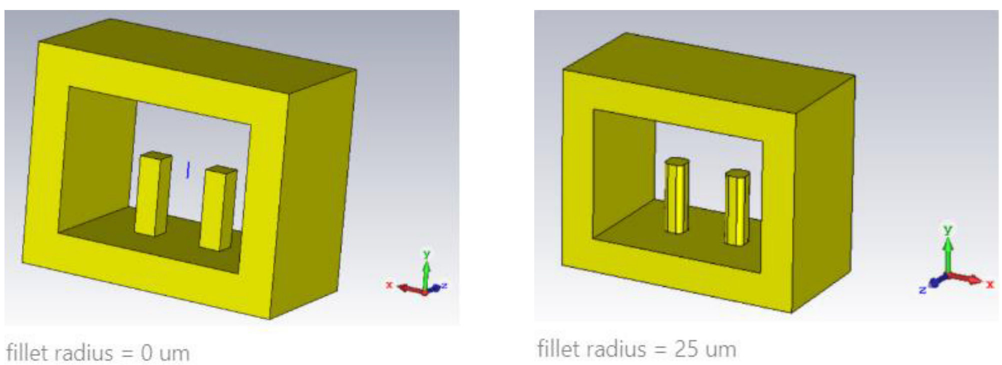

(a) (b)

Fig 1. Double corrugated waveguide without (a) and with fillet (b).

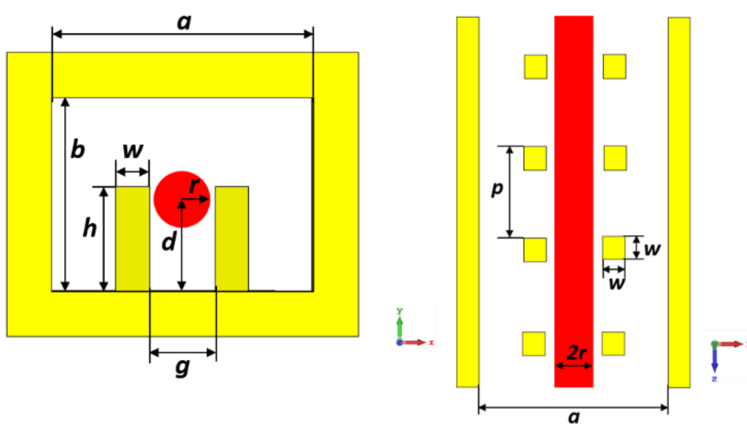

Fig 2. Double corrugated waveguide schematic with dimensions.

A small variation of the dimensions from the nominal value could affect dispersion and interaction impedance with possible performance degradation in the operation band. A sensitivity analysis of the variation of main dimensions is important to ensure the correct DCW behavior and to define the fabrication requirements. The sensitivity analysis will also permit to find possible mitigation solutions in case of deviation of performance from specifications, e.g. direction of variation of the beam voltage to compensate variations of the dispersion from the nominal one.

In the following, the sensitivity analysis on dispersion and interaction impedance as a function of the most critical dimensions such as the period *p*, the waveguide width *a*, the pillar height *b*, and beam position *d*, and area section, will be discussed for the DCW with square pillars in Fig (1a).

The dispersion and the interaction impedance computed by using the nominal dimensions given in Table 1 are shown in Fig 3. The dispersion is almost flat in a wide band including the operation band ensuring the synchronism with the electron beam. The interaction impedance is slightly higher than 1 Ω over the full frequency band. At D-band this value of interaction impedance is suitable for achieving up to 10 W output power.

Table 1. Nominal dimensions of the DCW

DCW width (*a*)	800 μm
DCW height (*b*)	588 μm
DCW period (*p*)	550 μm
Pillar height (*h*)	310 μm
Pillar width (*w*)	90 μm
Beam radius (*r*)	70 μm
Beam *y* position (*d*)	280 μm

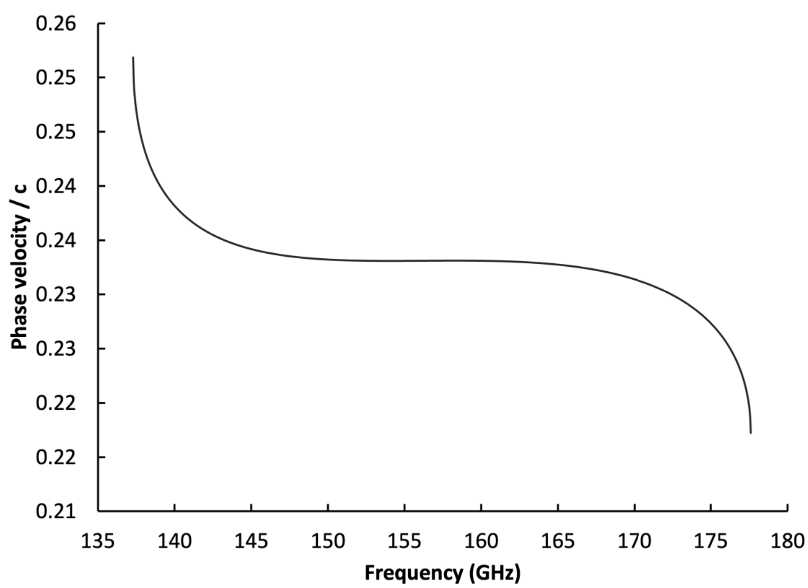

(a)

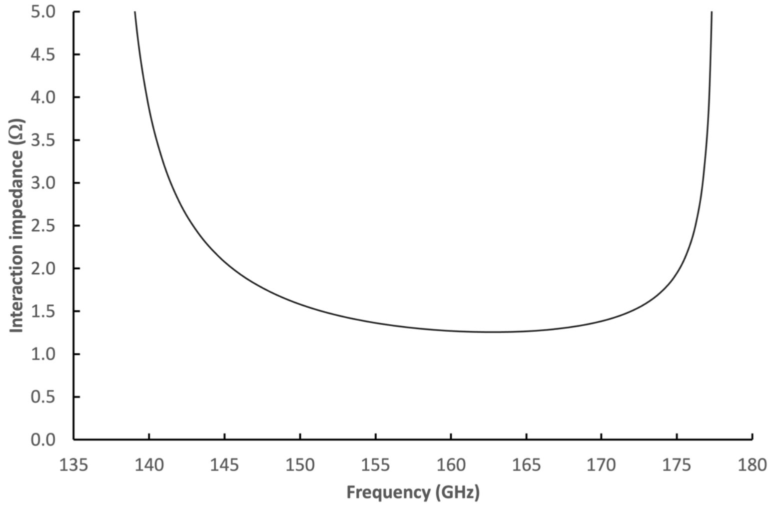

(b)

Fig 3. Normalized phase velocity (a) and Interaction impedance (b) of the DCW.

Figure 4 shows the dispersion curve with superimposed beam line at 13900 V. The wide overlap region provides very wide band behavior.

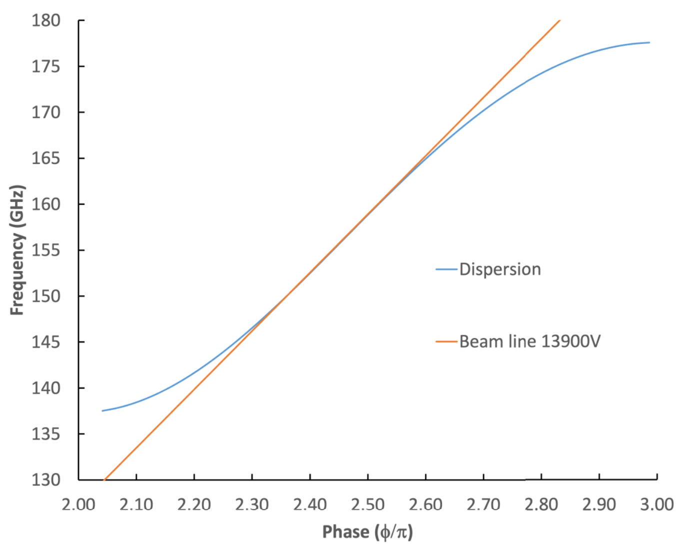

Fig 4. Dispersion curve with beam line computed at 13900 V beam voltage.

3 Double corrugated waveguide sensitivity analysis

Three most critical dimensions of the DCW are considered for the sensitivity analysis of dispersion and interaction impedance, specifically, height of the pillars *h*, DCW width *a* and period *p*. The position and the cross section of the electron beam are also important parameters for optimizing the performance. A specific sensitivity analysis to assess their impact on the interaction impedance will also be presented. In the following discussion, all the dimensions are referred to the nominal ones (Table 1), if not specified differently.

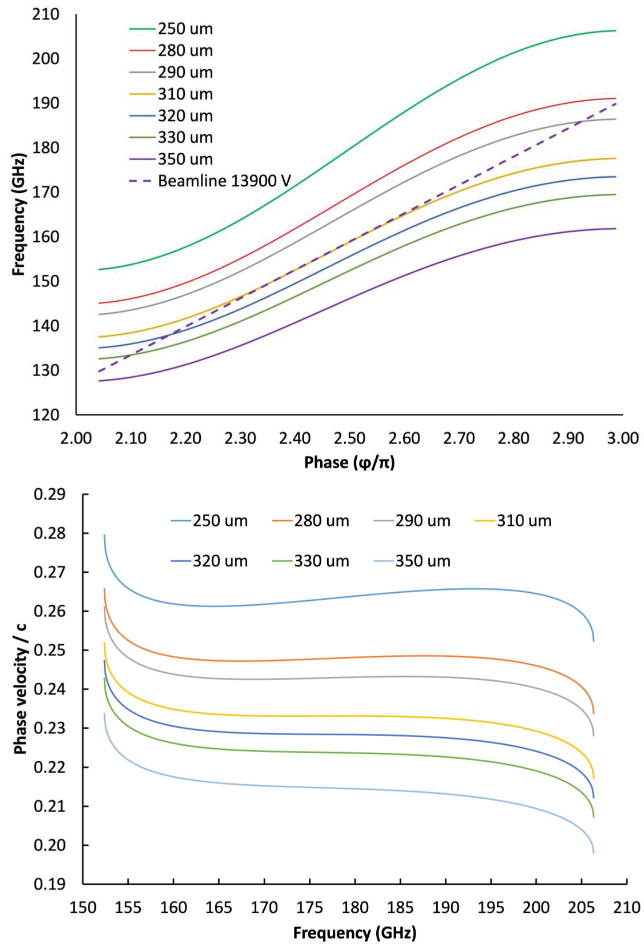

(a)

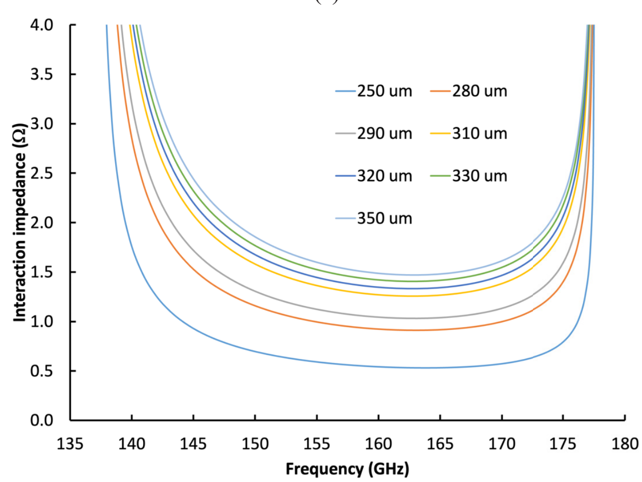

(b)

Fig 5. Dispersion curves (a) and interaction impedance (b) for pillar height '*h*' variation.

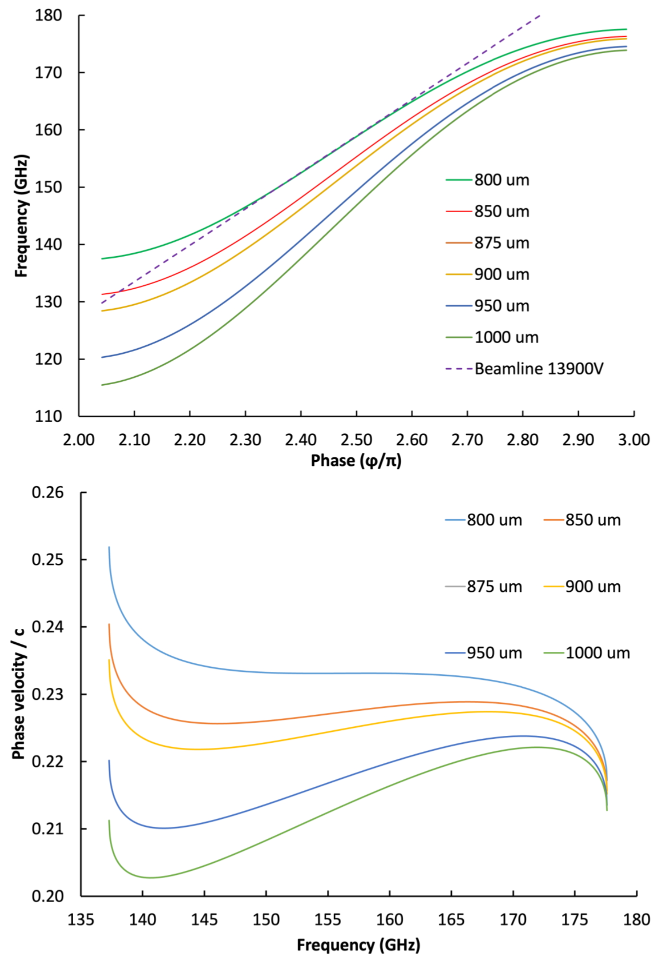

(a)

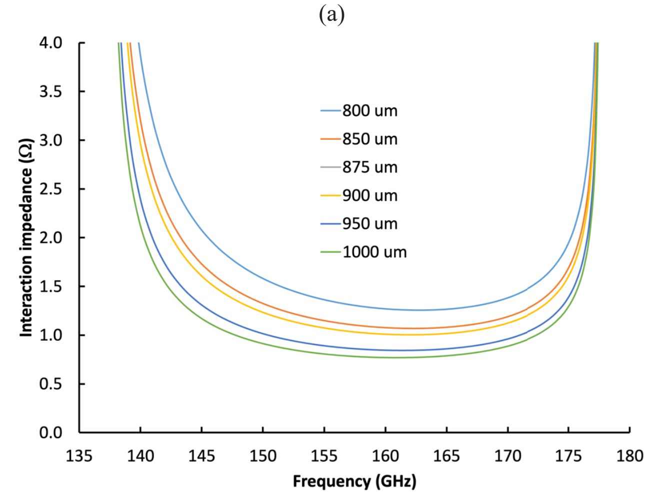

(b)

Fig 6. Dispersion curves (a), and interaction impedance (b) for waveguide width variation.

Figure 5 shows the effect of the variation of the height of the pillars h in the range 250-350 µm (nominal h = 310 µm). Figure 5(a) shows a substantial shift of the dispersion curve and a variation of the phase velocity, decreasing at the increase of the pillar height h (both the lower cutoff frequency and upper stop band frequency decrease). The interaction impedance (Fig 5(b)) increases at the increase of h with a variation higher than 50% of the nominal value. The variation of h has no specific impact on the operation center frequency.

Figure 6 shows the effect of the variation of the DCW width (a) in the range 800 -1000 µm (nominal a = 800 µm). Figure 6(a) shows the increase of the dispersion at the increase of DCW width (a) (the lower cut-off frequency decreases, upper stop-band frequency only slightly decreases), and a substantial reduction in the flatness of the phase velocity with related reduction of the synchronism frequency band with the beam voltage. Figure 6(b) shows a decrease of the interaction impedance at the increase of DCW width (a). Thus, Fig 6 demonstrates that the DCW width is very important for wide band behavior.

Figure 7 shows the sensitivity of dispersion to the DCW period p varied in the range 550-750 µm (nominal 550 µm). It is apparent from Fig 7(a) that at the increase of p, the upper stop band frequency decreases substantially while the lower cutoff frequency has only a slight variation. The increase of the phase velocity at the increase of p is relevant. This is confirmed by the relation of p with the beam voltage V_0 for a given frequency f [12]:

$$p = \frac{\phi 5.93 * 10^5 \sqrt{V_0}}{2f} \tag{1}$$

where f is the frequency, and ϕ is the phase shift.

To reduce the beam voltage, the period of the DCW has to be reduced, with possible fabrication constraints.

It is apparent from Fig 7(b) that the interaction impedance increases at the increase of the period p. The accuracy of the length of the period is very important due to the substantial variations of phase velocity and interaction impedance almost flat at the change of the period. It may be noted that the dispersion remains flat. However, in case of a variation, an adjustment in synchronism may be permitted by varying the beam voltage.

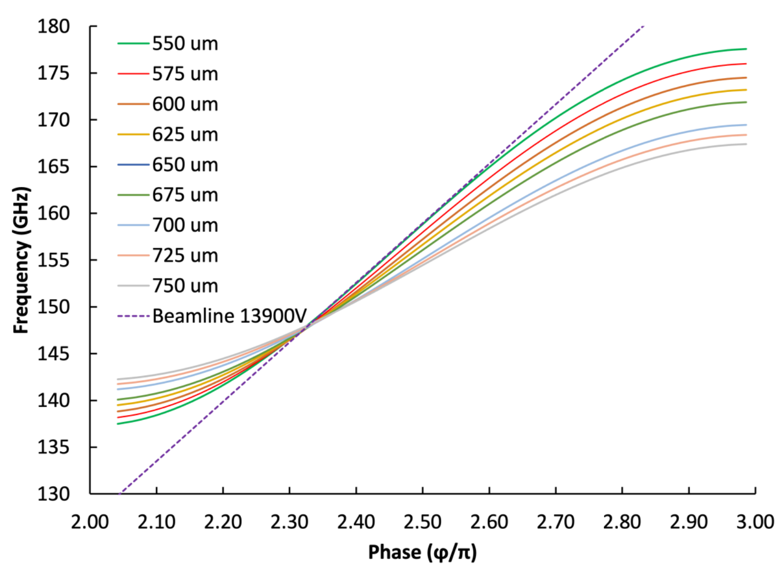

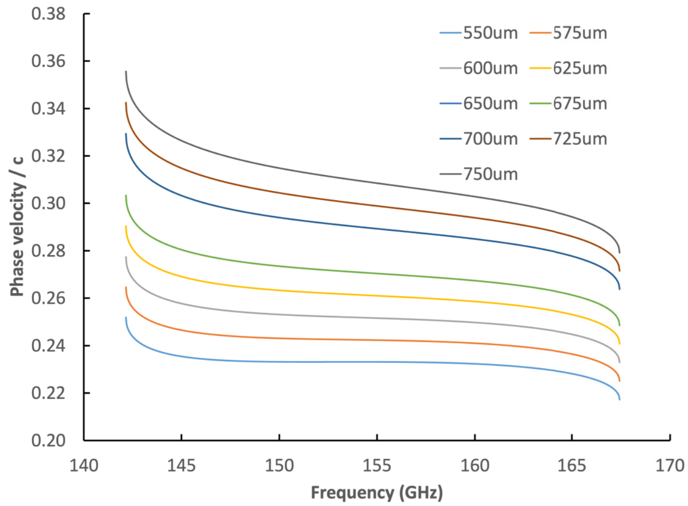

(a)

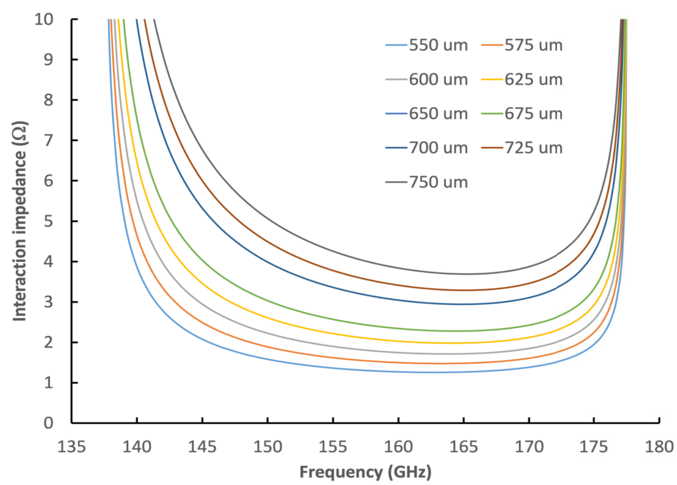

(b)

Fig 7. Dispersion curves (a), and interaction impedance (b) for period variation.

The electron beam travels between the two rows of pillars, as shown in Fig 2. The horizontal position is fixed at the center of the two pillar rows. The vertical position of the beam center is set to expose the electron beam to the region where the electromagnetic field is more intense. The position of the electron beam has no effect on the dispersion, that will not be considered in the following.

Figure 8 shows the variation of the average interaction impedance computed on the beam cross section. As expected, a larger area of the beam cross-section and the proximity with the pillars increase the average interaction impedance.

Figure 9 shows the interaction impedance calculated at the center of the electron beam as a function of the vertical position *d* of the beam center, varied in the range 250-350 µm (nominal *d* = 280 µm). One may note the region of the minimum variation at a location where the beam is close to the nominal position or lower. When the beam position is higher than the nominal position, the interaction impedance reduces due to the low electric field intensity. This behaviour suggests that a position of the beam lower than its nominal position does not have a significant effect on the interaction impedance.

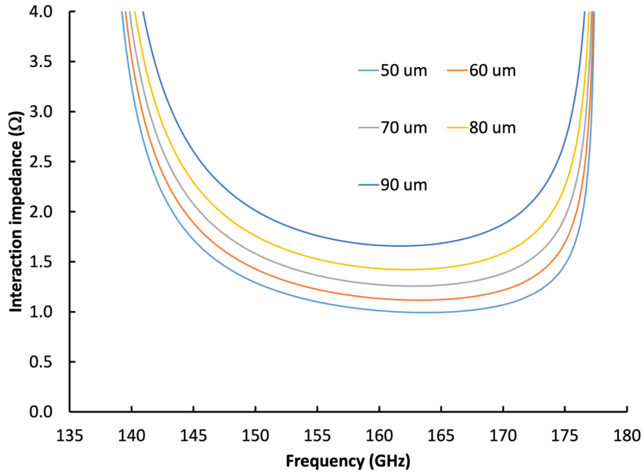

Fig 8. Interaction impedance as a function of the beam radius (*r*) (cross section area).

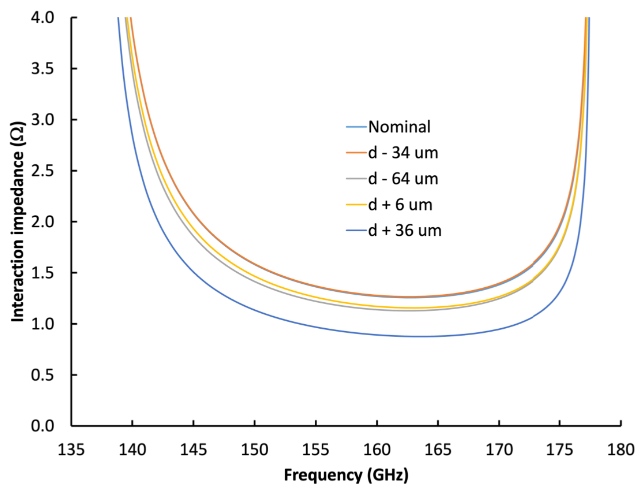

Fig 9. Interaction impedance as a function of the electron beam center (*d*) computed with reference to the nominal position $d = 280$ µm.

Table 2. Effect of dimension variation on the DCW design parameters

Parameter	DCW width *a*	Pillar period *p*	Pillar height *h*	Beam radius *r*
Dispersion	Direct	Inverse	Inverse	-
Bandwidth	Direct	Inverse	Inverse	-
Start frequency	Inverse	Direct (slightly)	Inverse	-
Stop frequency	Inverse (slightly)	Inverse	Inverse	Direct
Interaction impedance	Inverse	Direct	Direct	-
Beam voltage	inverse	Direct	Inverse	-

The graphs in Figs 5-9 provide very useful general guidelines to design a DCW valid for any frequency band. Table 2 summarizes the direction of change of the various design parameters as a function of the variation of the main DCW dimensions. As an example, to increase the interaction impedance, the period should be longer, but at the expense of the bandwidth. Obviously, to define the final dimensions of the DCW, it will be necessary to perform 3D electromagnetic simulations.

4 Sensitivity analysis as a function of fillet radius

Fillets may be introduced in the pillar geometry (Fig 2b) either as a design approach to simplify the fabrication or due to eventual fabrication errors. Simulations were carried out to estimate the effect of fillets on dispersion, interaction impedance and beam voltage. The fillet radius (r_f) on pillar edges was varied in the range 0 (nominal value in case of sharp edges) - 25 µm. Figure 10 shows that the presence of fillets caters a slight variation of the phase velocity that can easily be compensated with a minor variation of beam voltage. It is worth mentioning here that the interaction impedance is not affected due to the fillets (Fig 11). This study confirms the robustness of the design of the DCW structure to variations of the shape of the pillars [13]

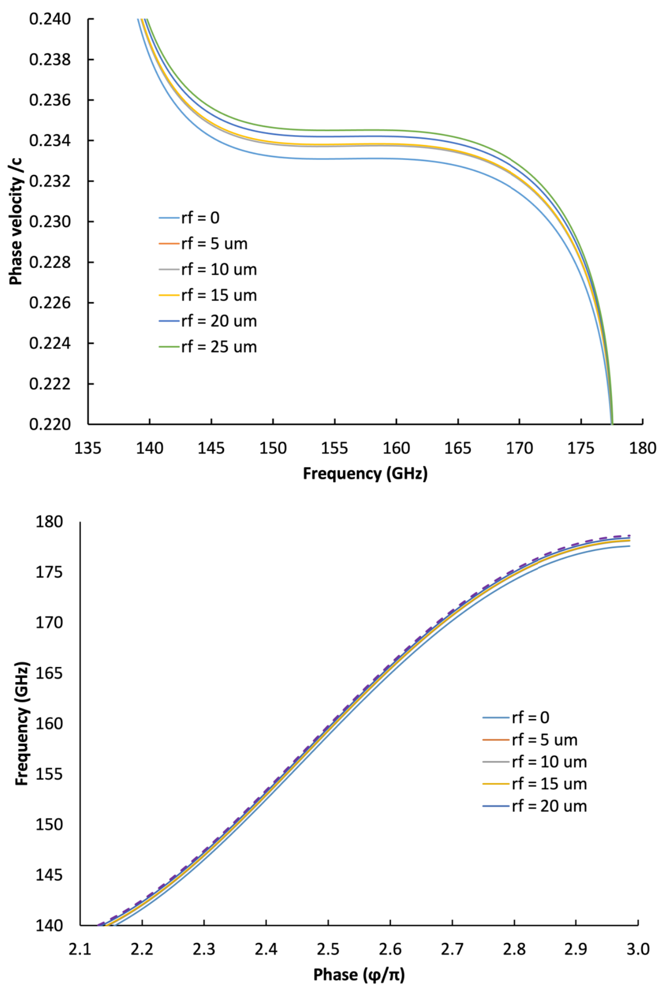

Fig 10. Normalized phase velocity as a function of the fillet radius r_f.

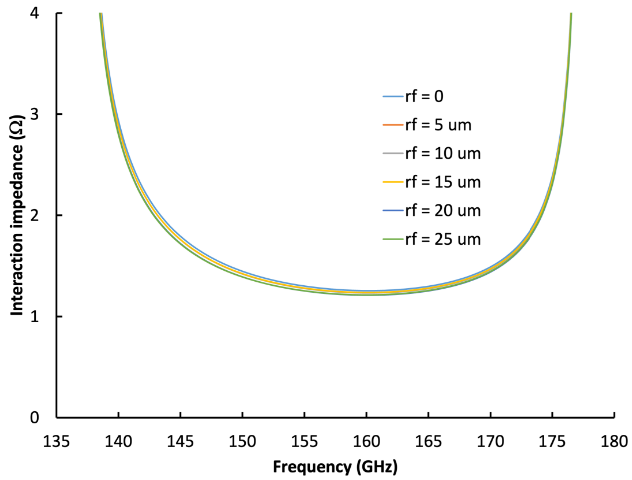

Fig 11. Interaction impedance as a function of the fillet radius r_f.

5 Conclusions

Sensitivity analysis of the geometry parameters is a powerful methodology to predict the deviation of the cold parameters from the nominal specifications and optimize the dimensions of the DCW. Due to the size of the computational domain, it is very difficult to perform a sensitivity analysis by particle in cell simulations, but the information obtained by the sensitivity analysis of the cold parameters permits to predict possible improvement of performance and fabrication requirements. The study highlights that some dimensions are more sensitive to fabrication tolerance than others and eventual deviations could be corrected by tuning the beam voltage. The presence of fillets in the pillars only slightly affects dispersion and interaction impedance, giving flexibility and allowing a margin of error for the pillar shape.

Acknowledgement

The research described in this publication was made possible by the DLINK- D-band Wireless Link with Fibre Data Rate project funded by EPSRC grants EP/S009620/1.

References

1. Dhillon S S, Vitiello M S, Linfield E H, Davies A G, Hoffmann M C, Booske J, Paoloni C, Gensch M, Weightman P, Williams G P, Castro-Camus E, Cumming D R S, Simoens F, Escorcia-Carranza I, Grant J, Lucyszyn S, Kuwata-Gonokami M, Konishi K, Koch M, Schmuttenmaer C A, Cocker T L, Huber R, Markelz A G, Taylor Z D, Wallace V P, Zeitler J A, Sibik J, Korter T M, Ellison B, Rea S, Goldsmith P, Cooper K B, Appleby R, Pardo D, Huggard P G, Krozer V, Shams H, Fice M, Renaud C, Seeds A, Stöhr A, Naftaly M, Ridler N, Clarke R, Cunningham J E, Johnston M B, The 2017 terahertz science and technology roadmap, *J Phys D: Appl Phys*, 50(2017)043001; doi. 10.1088/1361-6463/50/4/043001.
2. Paoloni C, Sub-THz wireless transport layer for ubiquitous high data rate, *IEEE Commun Mag*, 59(2021)102–107.
3. Maiwald T, Li T, Hotopan G.-R, Kolb K, Disch K, Potschka J, Haag A, Dietz M, Debaillie B, Zwick T, Aufinger K, Ferling D, Weigel R, Visweswaran A, A review of integrated systems and components for 6g wireless communication in the d-band, *Procd IEEE*, 111(2023)220–256.
4. Paoloni C, Gamzina D, Letizia R, Zheng Y, Luhmann N C (Jr), Millimeter wave traveling wave tubes for the 21st century, *J Electromagn Waves Appl*, 35(2021)567–603.
5. Gamzina D, Himes L G, Barchfeld R, Zheng Y, Popovic B K, Paoloni C, Choi E, Luhmann N C, Nano-cnc machining of sub-THz vacuum electron devices, *IEEE Trans Electron Devices*, 63(2016)4067–4073.

6. Basu R, Rao J M, Le T, Letizia R, Paoloni C, Development of a D-band traveling wave tube for high data-rate wireless links, *IEEE Trans Electron Devices*, 68 (2021)4675–4680.
7. Andre F, Racamier J, Zimmermann R, Le Q T, Krozer V, Ulisse G, Minenna D F G, Letizia R, Paoloni C, Technology, assembly, and test of a W-band traveling wave tube for new 5g high- capacity networks, *IEEE Trans Electron Devices*, 67(2020)2919–2924.
8. Wenqiang L, Yi J, Quanfeng Z, Peng H, Linlin H, Lei Y, Hongbin C, Development of D-band continuous-wave folded waveguide traveling-wave tube, in 2015 IEEE International Vacuum Electronics Conference (IVEC), pp 1–3, 2015.
9. Wang Z, Zhou Q, Gong H, Liao J, Wei Y, Duan Z, Liu H, Gong Y, Development of a 140-GHz folded-waveguide traveling-wave tube in a relatively larger circular electron beam tunnel, *J Electromagn Waves Appl*, 31(2017)1914–1923.
10. Field M, Kimura T, Atkinson J, Gamzina D, Luhmann N C, Stockwell B, Grant T J, Griffith Z, Borwick R, Hillman C, Brar B, Reed T, Rodwell M, Shin Y.-M, Barnett L R, Baig A, Popovic B, Domier C, Barchfield R, Zhao J, Higgins J A, Goren Y, Development of a 100-W 200-GHz high bandwidth mm-wave amplifier, *IEEE Trans Electron Devices*, 65(2018)2122–2128.
11. Paoloni C, Basu R, Billa L, Rao M, J, Letizia R, Ni Q, Wasige E, Al-Khalidi A, Wang J, Morariu R, Long-range millimetre wave wireless links enabled by travelling wave tubes and resonant tunnelling diodes, *IET Microw Antennas Propag*, 14(2020)2110–2114.
12. Mineo M, Paoloni C, Double-corrugated rectangular waveguide slow-wave structure for terahertz vacuum devices, *IEEE Trans Electron Devices*, 57(2010)3169–3175.
13. Mineo M, Paoloni C, Improved corrugation cross-sectional shape in terahertz double corrugated waveguide, *IEEE Trans Electron Devices*, 59(2012)3116–3119.

[*Received*: 28.04.2023, *revised recd*: 24.06.2023; *accepted*: 01.07.2023]

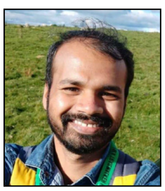

Jeevan M Rao received the Bachelor of Engineering (B.E) in Electronics and Communication Engineering from B.M.S College of Engineering, Bangalore, India in 2010, and M Tech. in Microwave Engineering from Kerala University, India in 2013. He worked for a short stint as a Senior Research Fellow (2013) at Microwave Tubes Research and Development Centre (MTRDC), Bangalore, India, where he worked on Gyrotrons. In 2014, he joined Bharat Electronics Limited (BEL), Bangalore, India as a Product Development Engineer, and continued there till 2018. During his career at BEL, he has successfully developed a number of high power Microwave Power Modules. Jeevan joined the School of Engineering, Lancaster University, UK, in November 2018 as Research Associate on the development of novel sub-THz traveling wave tubes.

Jeevan M Rao sadly passed away on 25th December 2020 at Bangalore, India.

Ms Rupa Basu received her Masters degree in High Power microwave Devices and System Engineering from AcSIR, India in 2013. She was a Senior Researcher Associate at the School of Engineering, Lancaster University. Her research is on design and fabrication of sub-THz travelling wave tubes. She is the recipient of the Best student paper award at IVEC 2020 for her research on D-band Travelling Wave Tube.

She has worked on design and development of helix travelling wave tubes for strategic applications at CEERI, India and Bharat Electronics, India. She has diverse experience of working in High Power microwave devices for space, defence and telecommunication industries.

Rosa Letizia (Senior Member, IEEE) is currently working as Senior Lecturer at the School of Engineering, Lancaster University, UK. She is also with the Cockcroft Institute of Accelerator Science and Technology, Warrington, UK. She is Senior Fellow of Advance Higher Education in UK. She has authored more than 120 journal papers and conference publications on millimetre wave travelling wave tubes, periodic structures, and other waveguide components design and fabrication. She has been an Associate Editor of IEEE Transactions on Electron Devices since 2020 and was a Royal Academy of Engineering/ Leverhulme Trust Senior Research Fellow in 2019-21.

Claudio Paoloni since 2012 has been full professor and Cockcroft Chair with the School of Engineering at Lancaster University. He was the Head of School of Engineering (2015-2022). He is Associate Editor of IEEE Transaction of Microwave Theory and Techniques and vice-Chair IEEE EDS Region 8. He was member at large of the Board of Governor of the IEEE Electron Devices Society. He was Chair of the IEEE Electron Devices Society Vacuum Electronics Technical Committee (2017 - 2020). He is IEEE Senior Member and Senior Fellow of the Higher Education Academy in the UK. He was Guest Editor in Chief of the Special Issue of IEEE Transaction on Electron Devices on Vacuum Electronics published in June 2023. He was coordinator of two European Commission Horizon 2020 projects, TWEETHER and ULTRAWAVE. He published about 260 reviewed articles. He is author of four book chapters. He has established at Lancaster University the “TWT Fab” a unique in Europe distributed laboratory for sub-THz Traveling Wave Tube fabrication.